An Experimental Study of Laminar Film Condensation with Stefan Number Greater Than Unity

by

R. L. Mahajan, AT&T- Bell Laboratories, Princeton, NJ 08540

T.Y. Chu, Sandia Laboratories, Albuquerque, NM 87185

D. A. Dickinson, AT&T- Bell Laboratories, Princeton, NJ 08540

ABSTRACT

Experimental laminar condensation heat transfer data is reported for fluids with Stefan number up to 3.5. The fluid used is a member of a family of fluorinated fluids developed in the last decade which have been extensively used in the electronics industry for soldering, cooling, and testing applications. Experiments were performed by suddenly immersing cold copper spheres in the saturated vapor of this fluid, and heat transfer rates were calculated using the quasi-steady temperature response of the spheres. In these experiments, the difference between saturation and wall temperature varied from 0.5 ℃ to 190 ℃. Over this range of temperature difference, the condensate properties vary significantly. For example, viscosity of the condensate varies by a factor of over 50. Corrections for the temperature dependent properties of the condensate therefore were incorporated in calculating the Nusselt number based on the average heat transfer coefficient. The results are discussed in light of past experimental data and theory for Stefan number less than 1. To the knowledge of the authors, this is the first reported study of condensation heat transfer for Stefan number greater than unity.

NOMENCLATURE

Bi	Biot number, $hD/2k_c$
c_p	specific heat at constant pressure
c_{pc}	specific heat of condensing surface
D	sphere diameter
g	gravitational acceleration
h	average heat transfer coefficient
h_{fg}	latent heat of vaporization
h'_{fg}	$h_{fg}(1 + 0.68\ S)$
k	thermal conductivity of condensate
k_c	thermal conductivity of copper
m_c	mass of condensing surface
Nu	average Nusselt number based on sphere diameter D
Nu_x	local Nusselt number, hx/k
Pr	condensate Prandtl number, $\mu c_p/k$)
S	Stefan or Jakob number, $c_p\Delta T/h_{fg}$
T	temperature
t	time
x	distance from the upper stagnation point for a sphere or from the leading edge for a plate

Greek Symbols

ΔT	difference between saturation temperature and sphere surface temperature
ΔT_o	difference between saturation temperature and constant surface temperature
δ	quasi-steady condensate film thickness
δ_{ss}	steady state condensate film thickness
μ	condensate dynamic viscosity
ν	condensate kinematic viscosity
ρ	density
τ	time

Subscripts

calc	calculated theoretical value
cp	constant property
exp	experimental
f	condensate
g	vapor
m	mean
ref	reference
sat	saturated
vp	variable property
w	sphere surface

1. Introduction

The classical analysis of laminar film condensation on vertical or inclined surfaces is due to Nusselt (1916). In that analysis the condensate film was assumed to be thin, and convective and inertia effects were considered to be negligible. Within the condensate film, gravity was balanced simply by the viscous force, and the temperature profile in the film condensate was assumed to be linear. From the analysis, the local heat transfer rate, Nu_x, was calculated to be

$$Nu_x = \left[\frac{(\rho_f - \rho_g)\ g\ h_{fg}\ x^3}{4\ \nu\ k\ (T_{sat} - T_w)}\right]^{1/4} . \quad (1)$$

Bromley (1952) performed an analysis using a non-linear temperature profile.

Rohsenow (1956) expanded the calculation to include the effect of liquid cross-flow within the film. The analysis, based on a control volume approach, resulted in a differential-integral equation which was solved by successive approximation. It was shown that the effect of the non-linear temperature distribution in the film can be accounted for by replacing h_{fg} in equation (1) by h^*_{fg}, where

$$h^*_{fg} = h_{fg}\left(1+\frac{3}{8}S\right)\left(1 - .1\ S - .0328S^2\right)/(1 - .1S)^2 . \quad (2)$$

For the range $0 < S < 1$, it was shown that equation (2) is very closely approximated by

$$h'_{fg} = h_{fg}\ (1 + .68S) . \quad (3)$$

The complete boundary solution, including the inertia and convection effects, was obtained by Sparrow and Gregg (1959). It was shown that except for very low Pr, Rohsenow's approximate analysis was quite adequate.

Koh et al. (1961) applied a boundary layer treatment to include the interfacial shear while Chen (1961) considered analytically the effect of thermal convection, inertia forces and interfacial shear. The Nusselt-Rohsenow approach was extended by Dhir and Lienhard (1971) to include axisymmetric bodies in non-uniform gravity. For a sphere of diameter D, the Nusselt number based on an average heat transfer coefficient was calculated to be

$$Nu = 0.785\left[\frac{(\rho_f - \rho_g)\ g\ h'_{fg}\ D^3}{4\ \nu\ k\ (T_{sat} - T_w)}\right]^{1/4} . \quad (4)$$

For a review of these and other earlier studies, see Merte (1973).

A study pertinent to the present investigation is an experimental investigation of quasi-steady laminar film condensation of steam on copper spheres by Dhir (1975). The average heat transfer data was obtained in the range of Stefan number 0.009 - 0.12 and was shown to be within ±13% of the steady state theoretical results of Dhir and Lienhard (1971) and Yang (1973).

All the studies of condensation heat transfer up to the present have been for relatively small sensible heat effects. The contribution of sensible heat is accounted for by correcting the latent heat of vaporization by a sensible heat term in the manner of equation (3). In these studies the correction is considered accurate for Stefan numbers up to 1. The recent study of Sadasivan and Lienhard (1987) showed that the correction factor is weakly dependent on *Pr*. The conventional view expressed in the literature is that this correction is adequate since *S* beyond unity exceeds the range of practical interest (Sadasivan and Lienhard, 1987).

In the last decade, new families of fluorinated fluids having Stefan numbers much greater than 1 in heat transfer applications have become widely used in various industries. Typical applications include electronic cooling and a mass soldering process, "condensation soldering." The process was invented as a method of supplying heat for soldering connector pins to printed circuit boards for telephone switching systems (Chu et al. 1974, Pfahl et al. 1975, Wenger and Mahajan 1979). In this method, articles to be soldered, having pre-deposited solder at joints, are immersed in a body of saturated vapor of a flourinated liquid with a typical saturation temperature of 215 ℃. The basic soldering machine consists of a vessel where vapor of the flourinated liquid is generated continuously by boiling. The vapor is condensed on a condensing coil near the top opening of the vessel. Because the vapor is much heavier than air, a stable body of saturated vapor can be maintained in the vessel between the boiling fluid layer and the condensing coil. The heat transfer to articles immersed in the vapor is rapid and uniform, with absolute control of the maximum temperature. Today, condensation soldering is used throughout the electronics industry.

During condensation heating of articles to be soldered, Stefan numbers as high as 3.5 are encountered. Therefore, it is of theoretical as well as practical interest to understand the effect of large sensible heat in condensation heat transfer. The present paper reports the results of a series of experiments carried out to observe film condensation for Stefan numbers up to 3.5. Condensation in this experiment is quasi-steady, and heat transfer rate is readily calculated by monitoring the temperature response of copper spheres suddenly immersed in saturated vapor of the fluorinated liquid.

2. Fluid Properties

The condensing fluid used in the present investigation is perfluorotriamylamine, $(C_5F_{11})_3N$, a member of the family of the perfluorinated inert liquids manufactured by 3M Co. The fluid is sold as *Fluorinert*[R] liquid and is commercially identified as FC-70. The physical properties of this fluid at 25 ℃, taken from the 3M Fluorinert Electronic Liquid Product Manual, are given in Table 1.

Table 1. Physical Properties of *FC-70*[R]

Typical Boiling Point ℃	215
Pour point ℃	-25
Average molecular weight	820
Surface tension, *dynes/cm*	18
Critical temperature, ℃	335 •
Critical pressure, *atmospheres*	10.2 •
Vapor pressure, *torr*	< 0.1
Solubility in water, *ppm*	8
Solubility of air, *ml/100ml*	22
Density, *g/ml*	1.93
Viscosity, *centistokes*	14.0
Specific heat, *cal/g-*℃	0.25
Heat of vaporization, *cal/g*	16
Thermal conductivity, *mW/cm*^{2}*-(*℃*/cm)*	0.69 •
Coefficient of expansion, *ml/ml-*℃	0.0010

• Estimated

R Trademark

The properties of this fluid that are of significance in determination of the film condensation heat transfer rate are the kinematic viscosity, thermal conductivity, specific heat, density, and heat of vaporization. Some of these are strongly dependent on temperature. For example, data provided by 3M Co. on measurements of viscosity (Table 2) indicate that for temperature over the range from room temperature to the boiling point of the liquid, the dynamic viscosity varies by as much as a factor of approximately 54. A least squares fit of the measured data resulted in the correlation of kinematic viscosity as a function of temperature,

$$\log \log (\nu + .90825) = (14.1226 - 5.69327 \log T) \quad (5)$$

where T is the temperature (K) and ν is dynamic viscosity (*centistokes*). The general form of this correlation is that recommended by ASTM Standard D 341-77, "Viscosity-Temperature Charts for Liquid Petroleum Products". The equation fitted the data in Table 2 to an accuracy of ±3%.

Table 2. Liquid Viscosity as a Function of Temperature

Temperature ℃	Measured Value of Viscosity, Centistokes
24	11.88
30	8.61
40	5.87
60	2.88
80	1.65
100	1.09
110	0.91
120	0.76
130	0.66
140	0.57
150	0.50
173	0.38
216	0.25

The measurements of k, ρ, and c_p as a function of temperature were obtained at AT&T's Thermal Engineering Laboratory at Bell Laboratories, Princeton. The best fit correlations describing the temperature dependencies of these properties are

$$k = 0.7242718 - 6.353033 \times 10^{-4}\, T \quad (6)$$

$$c_p = 2468938 + 1.51426 \times 10^{-4}\, T + 1.285630 \times 10^{-7}\, T^2 \quad (7)$$

$$\rho_f = 1.970381 - 1.829488 \times 10^{-3}\, T \quad (8)$$

where k, c_p, ρ_f, and T are thermal conductivity in *mW/cm* - ℃, specific heat in *cal/g* - ℃, density in *g/ml*, and temperature in ℃, respectively. The correlations fit the experimental data to an accuracy of ±2%

3. Experimental Apparatus and Procedure

Condensation experiments were conducted using copper spheres with diameters of 25.4 *mm* and 50.8 *mm* as the condensing surface. A diagram of the experimental set-up and the sphere assembly details are shown in Figures 1 and 2 respectively. The body of the sphere was machined from copper and finished with a smooth surface. It was supported from the bottom on a stainless steel tube to prevent condensate on the tube surface from running onto the sphere, and a ceramic insulator was used to separate the two pieces. A thermocouple used to measure the sphere temperature was positioned at the sphere center, with the leads running through the ceramic and through the stainless steel tube. Epoxy was used to support the thermocouple bead, which was held in place against the copper by the weight of the sphere. Epoxy was also used as a seal where the ceramic entered both the sphere and the steel tube.

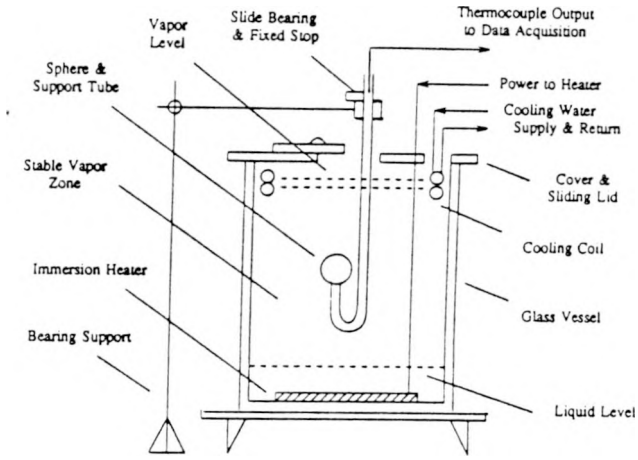

FIGURE 1. Experimental Apparatus

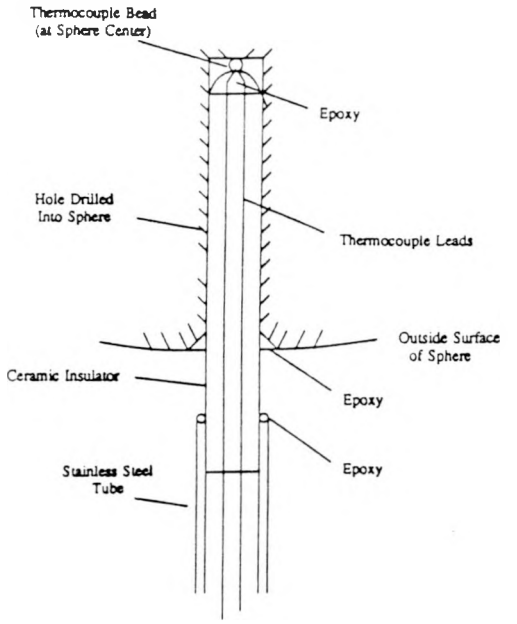

FIGURE 2. Details of Sphere Assembly

The vessel used to contain the sphere and condensing vapor was a cylindrical glass jar with height 46 *cm* and diameter 30 *cm*, as shown in Figure 1. Electric resistance immersion heaters were used to boil the liquid in the base of the jar and water cooled coils at the top were used to continuously condense the vapor, so that a region of saturated vapor was set up when the apparatus was fully heated and operating at steady state. Air filled the space above the saturated vapor zone. Power input to the heaters was adjustable using a variac. The jar was fitted with a stainless steel cover, with a smaller removable cover to allow the sphere to be inserted into the vapor. Hence the entire system was at atmospheric pressure. An equipment stand fitted with a slide bearing was used to hold the stainless steel tube supporting the sphere, with a stop clamped to the tube to fix the vertical position of the sphere within the vapor volume. This arrangement allowed manual insertion of the sphere to be fast, smooth, and repeatable. At the beginning of each run a thermocouple was used to read the actual vapor temperature T_{sat} to be used in the data reduction.

To begin an experimental run, steady state was first established in the jar. The heater power was adjusted so that the vapor/air interface was at the top turn of the condensing coils. This allowed the insertion of the sphere and resulting condensation to have a minimal effect on the vapor height, thus minimizing turbulence at the vapor/air interface and any intermixing of air into the vapor zone. Consistent with the past observations of Chu et al. (1975), the interface was observed to be well defined and stable. Temperature measurements were started just as the sphere, normally at room temperature, was lowered through the cover into position and continued until the sphere temperature was within a few degrees of T_{sat}. A data acquisition system was used to read the sphere temperature at pre-programmed time intervals, selected as 0.5 seconds for both sphere sizes. This interval was long enough to allow negligible error due to variation in the actual time interval used by the acquisition system as well as short enough to allow accurate determination of dT_w/dt at a given measured temperature T_w.

Profiles for T_w and dT_w/dt at the start of a run are shown in Figure 3. A transient period occurs as the sphere enters the vapor and the condensate film is established, followed by the period of quasi-steady condensation, during which a continuous condensate film was observed. As the run proceeds the temperature asymptotically approaches T_{sat}.

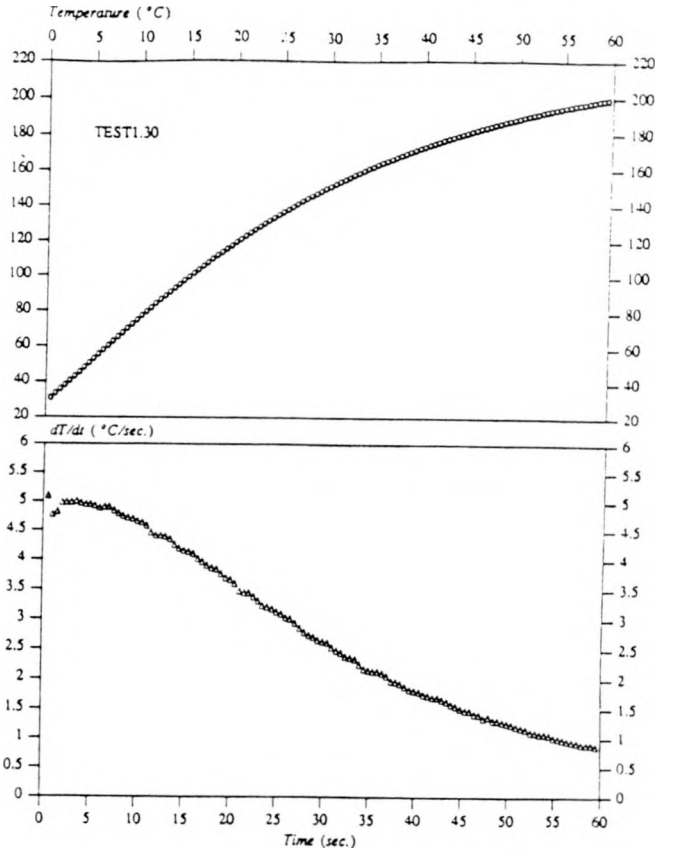

FIGURE 3. (a) Temperature vs. Time, (b) Rate of Temperature Rise vs. Time

4. Data Reduction and Analysis

4.1 Experimental Nusselt Number

A Fortran program was written to process the experimental data, which consisted simply of the temperature measurements at equal time intervals. The heat transfer coefficient h, at a given measured wall temperature, T_w, was determined using the lumped capacity relation,

$$m_c\, c_{pc}\, (dT_w/dt) = hA\,(T_{sat} - T_w) \quad . \tag{9}$$

The experimental Nusselt number Nu_{exp} is then

$$Nu_{exp} = hD/k \quad . \tag{10}$$

The error introduced using equation (9) is negligible if Bi is less than 0.4 (Dhir, 1975). For all the data to be presented Bi is less than 0.05, so the temperature of the sphere can be assumed uniform.

The rate of temperature rise, $dT_w/dt = \Delta T_w/\Delta t$ was calculated using at least two time intervals (1 second) to ensure sufficient accuracy for ΔT_w. At the beginning of a run the rate of temperature rise is about 5 °C/s with the 25.4 *mm* sphere. The accuracy of the temperature measurement is ±0.1 °C, so the accuracy of the calculation for h and Nu_{exp} is approximately ±5%. At higher sphere temperatures, with slower heating rate, additional time intervals are added to ensure that ΔT_w is at least 2 °C. The wall temperature was taken to be the average of the initial and final temperatures. This was used rather than an actual intermediate measurement of temperature to allow the use of odd numbers of intervals. The difference between the average and actual intermediate temperature was typically less than 0.1 °C.

4.2 Calculated Nusselt Number

In this experimental investigation, the film Reynolds number did not exceed 3, so that laminar film condensation analysis is applicable. For calculation of the theoretical Nusselt number, it must be determined whether the experiment is truly quasi-steady. Furthermore, a relationship between the quasi-steady and steady state calulations needs to be obtained. Dhir (1975) determined the relative liquid film thicknesses for the quasi-steady and steady state conditions and estimated the agreement that could be expected between the measured heat transfer coefficients for the two cases. For a vertical flat plate, local steady state film thickness is

$$\delta_{ss} = \left[\frac{4\nu k \Delta T_0 x}{g(\rho_f - \rho_g)h_{fg}'}\right]^{1/4} \tag{11}$$

It was shown by Dhir that the governing equation for the quasi-steady film thickness δ can be written as

$$\left[\frac{g(\rho_f-\rho_g)h'_{fg}}{\nu k\Delta T(t)}\right]\delta^3\frac{\partial\delta}{\partial x}=1+\left\{\left[\frac{dT_w}{dt}\frac{1}{\Delta T(t)}\frac{\delta^2}{\alpha}\right]\times\left[\frac{5}{8}+\frac{h_{fg}}{4c_p\Delta T(t)}\right]\right\} \quad (12)$$

For a sphere, the term g can be replaced by an effective gravitation as derived by Dhir. If the entire right hand side is treated as a constant and the left hand side is integrated, then

$$(\delta/\delta_{ss})^4=1+\left\{\left[\frac{dT_w}{dt}\frac{1}{\Delta T(t)}\frac{\delta^2}{\alpha}\right]\times\left[\frac{5}{8}+\frac{h_{fg}}{4c_p\Delta T(t)}\right]\right\} \quad (13)$$

where δ_{ss} has been substituted using equation (11). The term in the curly brackets represents a ratio of dimensionless thermal diffusion constant and the sensible heat capacity of the film (Dhir, 1975). When this ratio is small, quasi- steady film thickness approaches the steady state value.

It was shown by Dhir that for steam condensing on a copper sphere the ratio δ/δ_{ss} is approximately 1.06 with the minimum value of S = 0.009, so that quasi-steady condensation should result in measured values of heat transfer coefficient within a few percent of those that would be obtained for steady state. For the present case with FC-70 condensing on a 25.4 mm sphere, with $(dT_w/dt)(1/\Delta T)$ approximately 0.035 s^{-1} (from the measured data), an intermediate value of S = 1.5, approximate film thickness of $1.0\times10^{-4}m$ (from equation 11), and thermal diffusivity of the condensate of $3.3\times10^{-8}m^2/s$, we have δ/δ_{ss} = 1.008. The agreement is considerably closer than that with steam, due partly to the slower heat transfer with this fluid, but mainly due to the much larger value of S. Clearly the steady state calculations can be used to accurately predict the quasi-steady condensation heat transfer rates for the fluid used in this investigation.

For determining the theoretical values of Nusselt number, Nu_{calc}, the full boundary layer solutions of Sparrow and Gregg (1959) can be used. However, as noted there, for Pr > 10, the full boundary layer solutions are very close to the approximate calculations of Rohsenow (1956). For FC-70 condensate, Pr varies from 320 at room temperature (25 ℃) to approximately 8 at the saturation temperature (215 ℃). Equations (2) and (4) are therefore appropriate for obtaining theoretical estimates of Nu. Also note that although equation (3) is prescribed in Rohsenow's paper for use in the range $0 < S < 1$, our calculations of h using both equations (2) and (3) for values of S much greater than 1 (we performed calculations for S up to 20) indicate that difference between the two calculations is at the most 0.5%. In the results to follow, we have therefore chosen to use the simplified equation (3) in conjunction with equation (4) to calculate Nu_{calc}.

The experimental heat transfer data will be presented relative to the theoretical values calculated in the manner above in terms of the ratio Nu_{exp}/Nu_{calc}. The wall temperature will be presented in terms of the Stefan number, S.

5. Results and Discussion

Results for three runs using the smaller sphere are shown in Figure 4. The temperature T_{ref} used for calculation of fluid properties was the average of T_w and T_{sat}. Attention will be focused on TEST1.30, which is a typical run with the sphere initially at room temperature, corresponding to an initial Stefan number of nearly 3.5.

The sequence of points measured during the run moves to the left as the sphere heats up. It appears that the Nusselt number ratio is fairly constant for Stefan numbers between approximately 0.3 and 2.3 and drops off at both ends of this range. There are a number of non-ideal effects that contribute to this behavior, including disturbance to the vapor zone due to insertion of the test object, the effect of property variation, and effect of non-condensable gases. Each of these effects will be addressed in the following sections.

5.1 Effect of Thermal Transients and Initial Disturbance

The time required to achieve steady state after suddenly dropping the temperature of a sphere already immersed in saturated vapor was obtained by Sparrow and Siegel (1959) as

$$t_{ss}=\left[\frac{h_{fg}\rho_f\mu x}{g(\rho_f-\rho_g)k\Delta T_0}\right]^{1/2}\times\left[1+\frac{c_p\Delta T_0}{2h_{fg}}\right] \quad (11)$$

For the present case with FC-70, t_{ss} is approximately 0.25 to 0.50 seconds. However, this accounts for the thermal transient only and does not include the effect of lowering the sphere into the vapor as done in these experiments. The disturbance of the vapor zone results in a transient period that is considerably longer, as discussed below, so that the thermal transient alone cannot be observed in the measured data.

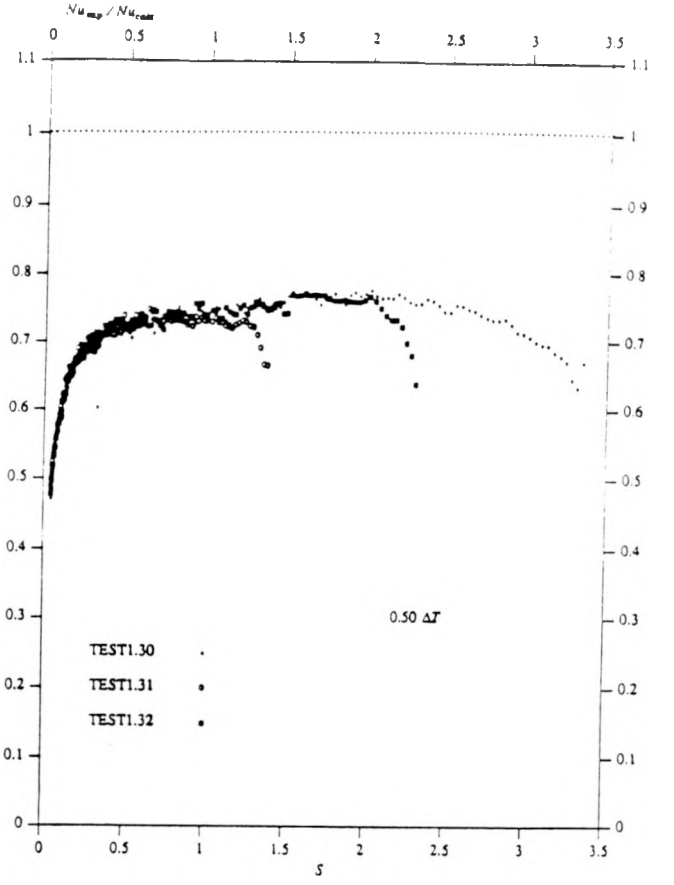

FIGURE 4. Comparison of Runs With Different Initial Sphere Temperatures.

When the interface between the vapor and air is disturbed, the vapor and air become inter-mixed creating a fog-like zone surrounding the entry region. This fog also follows the sphere into the vapor zone. Therefore, for the first few seconds of the experiment the condensation rate is expected to be lowered by the presence of air and possibly water vapor as non-condensable gas. A measure of the disturbance time is obtained by performing runs with elevated initial temperatures and observing the time required for the data to merge into that for the run with ambient initial temperature. Typical results are shown Figure 4. Runs TEST1.31 and TEST1.32 correspond to initial sphere temperatures of 100 ℃ and 150 ℃, respectively. For both the runs the insertion transients are clearly visible. They occur over a time period of approximately 4 seconds (8 data points), independent of initial temperature, and exhibit a very steep slope approaching the ambient initial temperature run. The decrease in the Nusselt number ratio at high S for the ambient initial temperature run occurs over a much longer period of time and is not solely an effect of initial transient. This is discussed in detail below.

5.2 Effect of Property Variations

The decline in Nusselt number ratio for Stefan number greater than about 2.3 can be attributed to the effect of viscosity variation in the condensate film. For example, for the test data shown in Figure 4, S = 2.3 corresponds to T_w = 96 ℃. The viscosity varies across the condensate film by a factor of about 5. For S = 3.35, corresponding to T_w = 30.8 ℃, the variation is a factor of about 34.

The standard way of correcting for property variations is to use a film temperature defined as

$$T_{ref}=T_w+C\Delta T \quad (12)$$

where the constant C takes on values between 0.23 to 0.33 (Minkowycz and Sparrow 1966, Poots and Miles 1967, Denny and Mills 1969). However, this correction is for water and the associated property variation is relatively small. The correction with C = 0.31 is shown in Figure 5. For larger property variation, the power law correction factor based on viscosity ratio is adapted to correct the calculated Nusselt number:

$$Nu_{vp}=Nu_{cp}\left(\frac{\mu_m}{\mu_w}\right)^n \quad (13)$$

where subscript m denotes the mean temperature (C = 0.5) across the boundary layer. This method has been successfully used for laminar forced flow in tubes. The exponent n takes on a value of either 0.11 (Yang, 1962) or 0.14 (Deissler, 1951).

With the power law correction using $n = 0.11$, the Nusselt number ratio approaches asymptotically a maximum value of about 0.87 at high S, as shown in Figure 5. Using the correction with $n = 0.14$, the ratio continues to rise with increasing slope. Note that the data corresponding to the initial disturbance period of 4 seconds has been included.

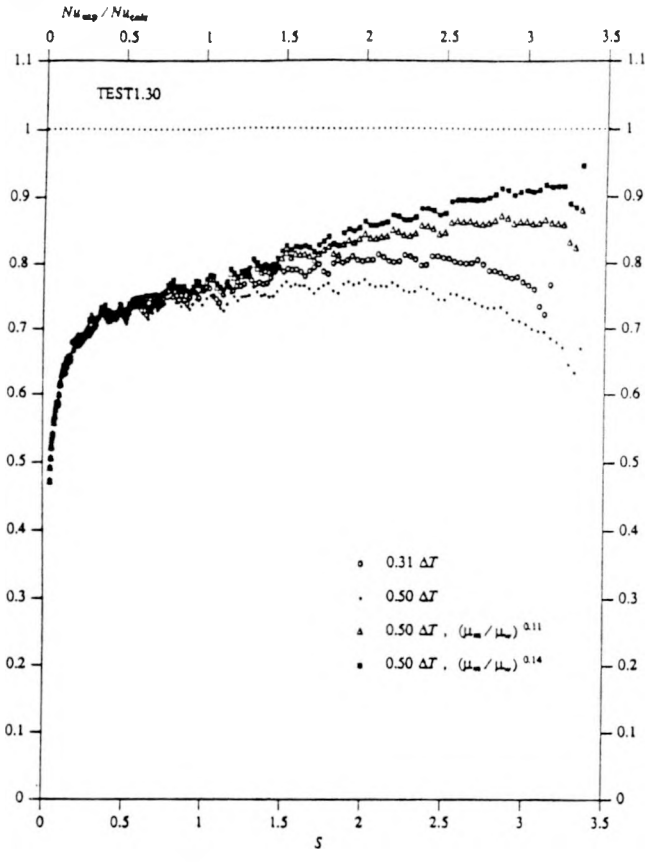

FIGURE 5. Effects of Reference Temperature and Viscosity Corrections

5.3 Effect of Noncondensable Components

The difference of about 10% between Nu_{exp} and Nu_{calc} using the power law correction (0.11 or 0.14) probably is due mainly to the presence of air which, as a noncondensible gas, impedes the motion of vapor to the condensing surface and hence reduces the rate of heat transfer. In addition, water vapor present at a concentration even as high as a 3% will have a condensing temperature less than 25 °C and hence also will be noncondensable over the full range of S.

The more or less linear decrease of the Nusselt number ratio with S in the range $0.3 < S < 3.3$ and the abrupt drop below $S = 0.3$ can be attributed to the fact that the working fluid FC-70 is not a single component fluid but a continuum of volatile components that condense over a range of temperatures. The results of distillation of a sample of FC-70 are plotted in Figure 6 in terms of temperature. The corresponding S is shown, assuming $T_{sat} = 215$ °C. As the sphere temperature increases during an experimental run, an ever increasing fraction of the vapor becomes noncondensable, thus decreasing the rate of heat transfer. An inspection of Figure 6 shows that 1% of low temperature volatiles become noncondensable at approximately 203 °C. For the sphere at this temperature, the correspoonding value of S is 0.22. This is very close to the value of S below which the heat transfer rate drops precipitously. Relatively small amounts of noncondensables can have a significant effect on condensation rates (Rose, 1969 and Felicione and Seban, 1973).

Experimental results for the larger sphere, with diameter 50.8 *mm*, show the same trends as observed with the smaller sphere. Some representative heat transfer results are compared to those for the smaller sphere in Figure 7.

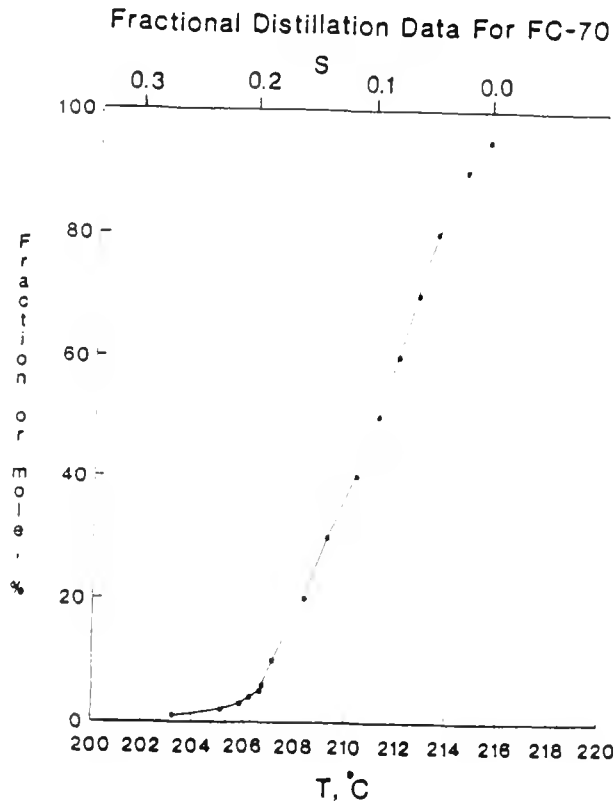

FIGURE 6. FC-70 Distillate Collected (% of Original Sample) as a Function of Temperature and Corresponding Stefan Number.

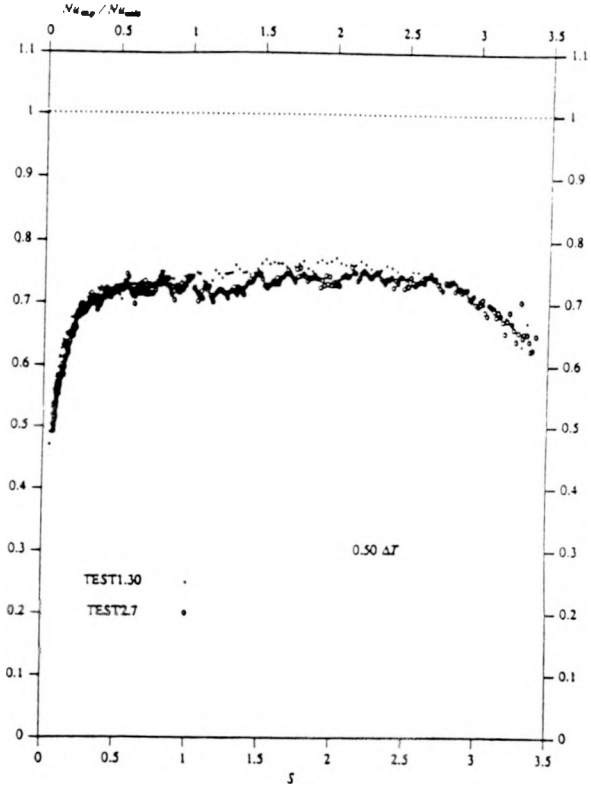

FIGURE 7. Comparison of Data for 1 inch (TEST1.30) and 2 inch (TEST2.7) Spheres

6. Concluding Remarks

1. Laminar film condensation results for Stefan numbers greater than unity have been presented. The fluid used, Flourinert FC-70 is one of the several similar fluids which are now routinely used in condensation soldering applications in the electronics industry.
2. For the fluid used, the ratio of dimensionless thermal diffusion time constant and sensible heat capacity is very small so that quasi-steady laminar condensation heat transfer results obtained by immersing copper spheres at room temperature in a body of hot saturated vapor are very close to the steady state heat transfer calculations.
3. Calculations indicate that for large *Pr* fluids, the simplified Nusselt-Rohsenow equations (1) and (2) recommended for use for $0 < S < 1$, can also be used to give accurate predictions of heat transfer rates for larger values of *S*.
4. The experimental heat transfer rates, when corrected for viscosity variations, are within 10% of the the theoretical values at large *S*. The deficit increases with decrease in *S*. This deficit is explained in terms of noncondensable components present in the vapor.
5. Experiments are planned in the future with ultra-pure single component distillate of FC-70 to further quantify the effect of the noncondensables on the experiments reported here.

References

1. Bromley, L.A., "Effect of Heat Capacity of Condensate", Ind. and Engr. Chem., Vol. 44, No. 12, 1952, p. 2966
2. Chen, M.M., "An Analytical Study of Laminar Film Condensation: Part I-Flat Plates", J. Heat Transfer 81, 1961, p. 48.
3. Chu, T.Y., Mollendorf, J.C., and Pfahl, R.C. Jr., "Soldering Using Condensation Heat Transfer," Proceedings of the Technical Program NEPCON, 1974, Anaheim.
4. Deissler, R. G., "Analytical Investigation of Fully Developed Laminar Flow in Tubes with Heat Transfer with Fluid Properties Variable Around the Radius", NACA TN 2410, 1951.
5. Denny, V.E. and Mills, A.F. "Non-Similar Solutions for Laminar Film Condensation on a Vertical Surface", Int. J. Heat Mass Transfer, Vol. 12, 1969, p. 965.
6. Dhir, V.K. and Lienhard, J.H., "Laminar Film Condensation on Plane and Axi-Symmetric Bodies in Non-Uniform Gravity", J. Heat Transfer, Trans. ASME, Series C, Vol. 95, No. 1, 1971, p. 97.
7. Dhir, V.K., "Quasi-steady Laminar Film Condensation of Steam on Copper Spheres", J. Heat Transfer, 1975, p. 347.
8. Felicione, F.S. and Seban, R.A., "Laminar Film Condensnation of a Vapor Containing a Soluble, Non-Condensing Gas," Int. J. Heat Mass Transfer, Vol. 16, 1973, p. 1601.
9. Koh, J.C.Y., Sparrow, E.M., and Hartnett, J.P., "The Two Phase Boundary Layer in Laminar Film Condensation", Int. J. Heat Mass Transfer, Vol. 2, 1961, p. 69.
10. Merte, H. Jr., "Condensation Heat Transfer", Advances in Heat Transfer, Vol. 9, 1973, Academic Press, p. 181.
11. Minkowycz, W.J. and Sparrow, E.M., "Condensation Heat Transfer in the Presence of Non-Condensables, Interfacial Resistance, Superheating, Variable Properties, and Diffusion", Int. J. Heat Mass Transfer, Vol. 9, 1966, p. 1125.
12. Nusselt, W., "Die Operflachenkondensation des Wasserdampfes," Z. Ver Deutsch, Ing., Vol. 60, 1916, pp 541 and 569.
13. Pfahl, R.C. Jr., Mollendorf, J.C., and Chu, T.Y., "Condensation Soldering," Welding Journal, Vol. 54, No. 1, 1975, p. 22
14. Poots, G. and Miles, R.G., "Effects of Variable Physical Properties on Laminar Film Condensation of Saturated Steam on a Vertical Flat Plate," Int. J. Heat Mass Transfer, Vol. 10, 1967, p. 1677.
15. Rohnsenow, W.M., "Heat Transfer and Temperature Distribution in Laminar Film Condensation," Trans Am. Soc. Mech. Engrs. 78, 1956, p. 1645.
16. Rose, J.W., "Condensation of a Vapor in the Presence of a Non-Condensing Gas", Int. J. Heat Mass Transfer, Vol. 12, 1969, p. 233.
17. Sadasivan, P. and Lienhard, J.H., "Sensible Heat Correction in Laminar Film Boiling and Condensation", Int. J. Heat Mass Transfer, Vol. 109, 1987, p. 545.
18. Sparrow, E.M. and Gregg, J.L. "A Boundary-Layer Treatment of Laminar-Film Condensation, J. Heat Transfer, Vol. 81, No. 1, 1959, p. 13.
19. Sparrow, E.M. and Siegel, R., "Transient Film Condensation," J. Applied Mechanics, Trans. ASME Series E, Vol. 81, No. 1, 1959, p. 120.
20. Wenger, G.M. and Mahajan, R.L., "Condensation Soldering Technology - Part I: Condensation Soldering Fluids and Heat Transfer", Insulation/Circuits, Sept. 1979, p. 131.
21. Wenger, G.M. and Mahajan, R.L., "Condensation Soldering Technology-Part II: Equipment and Production", Insultation/Circuits, Oct. 1979, p. 133.
22. Wenger, G.M. and Mahajan, R.L., "Condensation Soldering Technology-Part III: Installation and Application", Insulation Circuits, Nov. 1979, p. 13.
23. Yang, K.T., "Laminar Forced Convection of Liquids in Tubes with Variable Viscosity", J. Heat Transfer, Vol. 84, 1962, p. 353.
24. Yang, J.W., "Laminar Film Condensation on a Sphere", Heat Transfer, Vol. 95, No. 2, 1973, p.174